MENU 2007
11th International Conference
on Meson-Nucleon Physics and
the Structure of the Nucleon
September10-14, 2007
IKP, Forschungzentrum Jülich, Germany

# CHARGED PION PHOTOPRODUCTION AND SCALING

*H. Gao* [1]
Department of Physics and Triangle Universities Nuclear Laboratory
Duke University
Durham, NC 27516, U.S.A.

**Abstract**

The $\gamma n \to \pi^- p$ and $\gamma p \to \pi^+ n$ reactions are essential probes of the transition from meson-nucleon degrees of freedom to quark-gluon degrees of freedom in exclusive processes. The cross sections of these processes are also advantageous, for the investigation of oscillatory behavior around the quark counting rule prediction, since they decrease relatively slower with energy compared with other photon-induced processes. In this talk, we discuss recent results on the $\gamma p \to \pi^+ n$ and $\gamma n \to \pi^- p$ processes from Jefferson Lab experiment E94-104. We also discuss the CLAS g10 analysis on the $\gamma n \to \pi^- p$ process.

## 1 Introduction

The interplay between the nucleonic and partonic pictures of the strong interaction represents one of the major issues in contemporary nuclear physics. Although standard nuclear models are successful in describing the interactions between hadrons at large distances, and Quantum Chromodynamics (QCD) accounts well for the quark interactions at short distances, the physics connecting the two regimes remains unclear. In fact, the classical nucleonic description must break down once the probing distances become comparable to those separating the quarks. The challenge is to study this transition region by looking for the onset of some experimentally accessible phenomena naturally predicted by perturbative QCD (pQCD).

The simplest is the constituent counting rule (CCR) for high energy exclusive reactions [1] at fixed center-of-mass angles, in which $d\sigma/dt \propto s^{-n+2}$, with $n$ the total number of point-like particles and gauge fields in the initial plus final states. Here $s$ and $t$ are the invariant Mandelstam variables for the

[1] Science Drive, Box 90308, Durham, NC 27516, U.S.A.

total energy squared and the four-momentum transfer squared, respectively. Many exclusive reactions [2] at high energy and large momentum transfer appear to obey the CCR and in recent years, a similar trend, i.e. global scaling behavior, has been observed in deuteron photo-disintegration experiments [3] - [6] at a surprisingly low transverse momentum value of $\sim 1.1$ $(\mathrm{GeV/c})^2$.

The same dimensional analysis which predicts the quark counting rule also predicts hadron helicity conservation for exclusive processes at high energy and large momentum transfers. However, polarization measurements on deuteron photo-disintegration [7], recently carried out in Hall A at Jefferson Lab (JLab), show disagreement with hadron helicity conservation in the same kinematic region where the quark counting behavior is apparently observed. These paradoxes make it essential to understand the exact mechanism governing the early onset of scaling behavior. Towards this goal, it is important to look closely at claims of agreement between the differential cross section data and the quark counting prediction. Historically, the elastic proton-proton ($pp$) scattering at high energy and large momentum transfer has played a very important role. In fact, the re-scaled 90° center-of-mass $pp$ elastic scattering data, $s^{10}\frac{d\sigma}{dt}$ show substantial oscillations about the power law behavior. Oscillations are not restricted to the $pp$ sector; they are also seen in $\pi p$ fixed angle scattering [8].

Recently, a number of new developments have generated renewed interest in this topic. Zhao and Close [9] have argued that a breakdown in the locality of quark-hadron duality results in oscillations around the scaling curves predicted by the counting rule. They explain that the smooth behavior of the scaling laws arises due to destructive interference between various intermediate resonance states in exclusive processes at high energies. However, at lower energies this cancellation due to destructive interference breaks down locally and gives rise to oscillations about the smooth behavior. On the other hand, Ji *et al.* [10] have derived a generalized counting rule based on a pQCD inspired model, by systematically enumerating the Fock components of a hadronic light-cone wave function. Their generalized counting rule for hard exclusive processes include parton orbital angular momentum and hadron helicity flip, thus they provide the scaling behavior of the helicity flipping amplitudes. The interference between the different helicity flip and non-flip amplitudes offers a new mechanism to explain the oscillations in the scaled cross-sections. The counting rule for hard exclusive processes has also been shown to arise from the correspondence between the anti-de Sitter space and the conformal field theory [11], the so-called string/gauge duality. Brodsky *et al.* [12] have used this anti-de Sitter/Conformal Field Theory correspondence or string/gauge duality to compute the hadronic light front

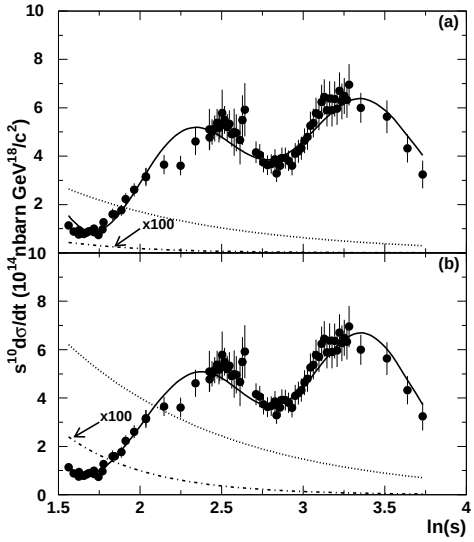


Figure 1: (a) The fit to $pp$ scattering data at $\theta_{cm} = 90°$ when helicity flip amplitudes are included as described in [13] . The parameters for the energy dependent phase was kept same as the earlier fit of Ralston and Pire [14]. The solid line is the fit result, the dotted line is contribution from the helicity flip term $\sim s^{-11}$, the dot-dashed line is contribution from the helicity flip term $\sim s^{-12}$. The $\sim s^{-12}$ contribution has been multiplied by 100 for display purposes.(b) The same data fitted to the form described in [13] but with the new more general parametrization of the Landshoff amplitude.

wave functions. This yields an equivalent generalized counting rule without the use of a perturbative theory.

Recently, it has been shown [13] that the generalized counting rule of Ji *et al.* [10] along with the Landshoff terms and associated interferences does a better job of describing the oscillations about the quark counting rule, in the $pp$ elastic scattering data at $\theta_{cm} = 90°$. Fig 1 shows the results of such a fit and also shows the explicit contributions from the $s^{-11}$ and $s^{-12}$ terms due to the helicity-flipping amplitudes in this approach. The value of $\Lambda_{QCD}$ was fixed at 100 MeV in the fit. This new fit is in much better agreement with the data. This is specially true in the low energy region ($s < 10$ GeV$^2$). The helicity flip amplitudes (mostly the term $\sim s^{-4.5}$) are significant at low energies and seem to help in describing the data at low energies. The contributions from helicity flipping amplitudes which are related to quark orbital angular momentum, seem to play an important

role at these low energies, which is reasonable given that the quark orbital angular momentum is non-negligible compared to the momentum scale of the scattering process. It is interesting to note that among the helicity flip amplitudes the one with the lower angular momentum dominates. Similarly the spin-correlation $A_{NN}$ [15] in polarized $pp$ elastic scattering data can be better described [13] by including the helicity flipping amplitude along with the Landshoff amplitude and their interference.

Exclusive $\gamma N \rightarrow \pi N$ processes are essential probes to study the transition from meson-nucleon degrees of freedom to quark-gluon degrees of freedom. The cross sections of these processes are also advantageous, for investigation of the possible oscillatory behavior around the quark counting prediction, since they decrease relatively slower with energy compared with other photon-induced processes. For the $\gamma\ n \rightarrow \pi^-\ p$ process, no cross section data exist above a photon energy of 2.0 GeV prior to the recent Jefferson Lab experiment E94-104 [16].

## 2 Jefferson Lab Experiment E94-104

Experiment E94-104 was carried out in Hall A [17] at the Thomas Jefferson National Accelerator Facility (JLab). The continuous electron beam, at a current around 30 $\mu$A and energies from 1.1 to 5.5 GeV, impinged on a 6% copper radiator and generated an untagged bremsstrahlung photon beam. The production data were taken with the 15 cm cryogenic liquid hydrogen (LH2) target for singles $p(\gamma, \pi^+)n$ measurement, and with the liquid deuterium (LD2) target for coincidence $d(\gamma, \pi^- p)p$ measurement. The two High Resolution Spectrometers (HRS) in Hall A were used to detect the outgoing pions and recoil protons. Two new aerogel Čerenkov detectors in the left spectrometer were constructed for this experiment to provide particle identification for positive particles, mainly pions and protons, since the time-of-flight technique fails at high momentum. Details of the Hall A spectrometers can be found [17].

Based on two-body kinematics, the incident photon energy was reconstructed from final states, i.e. the momentum and angle of the $\pi^+$ in the singles measurement, momenta and angles of the $\pi^-$ and $p$ in the coincidence measurement. A 100 MeV bin with the center of the bin 75 MeV from the beam energy, was chosen for the data analysis, where the multi-pion contribution was negligible. The data after background subtraction, with cuts on trigger type, coincidence timing, PID (particle identification), acceptance and photon energy, were compared to a modified Monte Carlo simulation code for this experiment based on MCEEP [18] with the same cuts on accep-

tance and photon energy. The raw cross section was extracted by comparing data and simulation. The distributions of acceptance, reconstructed momentum and photon energy were in good agreement with results obtained from simulations. Details on the simulation and the bremsstrahlung photon flux calculation can be found [19].

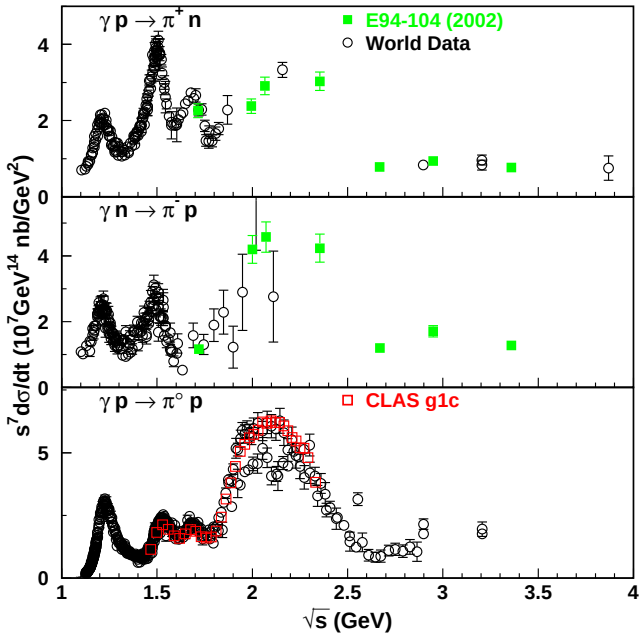


Figure 2: Scaled differential cross-section $s^7 \frac{d\sigma}{dt}$ as a function of center-of-mass energy $\sqrt{s}$ for a pion center-of-mass angles of 90°. The upper panel is for the $\gamma p \rightarrow \pi^+ n$ process, the middle panel is for the $\gamma n \rightarrow \pi^- p$ process, and the lower panel is for the $\gamma p \rightarrow \pi^0 p$ process. The green solid squares are results from [16], and results from Dugger *et al.* [20] on the neutral pion production are shown as red open squares. All other world data [22] are shown as black open circles.

The new results from E94-104 on $\gamma n \rightarrow \pi^- p$ greatly extend the existing measurements and exhibit, for the first time, a global scaling behavior at high energy for this reaction at 90°. The scaling behavior in $\pi^-$ production is similar to that in $\pi^+$ production. Results from experiment E94-104 also show dramatic change in the scaled differential cross-section from the $\gamma n \rightarrow \pi^- p$ and $\gamma p \rightarrow \pi^+ n$ processes in the center of mass energy between 1.8 GeV to about 2.4 GeV and a new resonance structure has been suggested by the data around 2.1 GeV at a pion center-of-mass angle of 90°. Fig. 2 shows the scaled differential cross-section $s^7 \frac{d\sigma}{dt}$ as a function of center-of-mass

energy $\sqrt{s}$ for a pion center-of-mass angles of 90° for three different channels. The upper panel is for the $\gamma p \to \pi^+ n$ process, the middle panel is for the $\gamma n \to \pi^- p$ process, and the lower panel is for the $\gamma p \to \pi^0 p$ process. The green solid squares are results from [16], the red open squares are results from Dugger *et al.* [20] on neutral pion production. In both the $\gamma p \to \pi^+ n$ and the $\gamma p \to \pi^0 p$ channel, one sees clearly the $\Delta$ resonance, the N(1500) and the N(1700) nucleon resonances. In the $\gamma n \to \pi^- p$ channel, while one also sees the $\Delta$ resonance and the N(1500) resonance, the existing data do not allow for a definitive statement about the N(1700) resonance in the scaled differential cross-section. There are two distinct features shown in the data for all three channels: broad resonance structure around a center-of-mass energy of 2.1 GeV, and a drastic fall-off of the differential cross-section in a narrow energy window of about 300 MeV. The second feature was first suggested by Jefferson Lab experiment E94-104 [16] (shown as green solid squares), and the $\pi^- p$ total scattering cross section data [21]. This has now been established by preliminary results from g10 on the $\gamma n \to \pi^- p$ which we will discuss next. The error bars for E94-104 include both statistical and systematic uncertainties, and neutral pion data [20] show only statistical uncertainties. All other world data are collected from Ref. [22] and are shown as black open circles.

The observed enhancement around 2.2 GeV might be related to some unknown baryon resonances. Several baryon resonances are predicted to be in this energy region by the constituent quark model [23], but have not been seen experimentally, i.e. the so called "missing resonances". There has been some evidence for the N(2070)$D_{15}$ resonance both from the $\pi^0$ [24] and $\eta^0$ [25] photoproduction off the proton. Recently, a global analysis [26] of charged pion photoproduction based on Regge model has been carried out for photon energies between 3 to 8 GeV where nucleon resonance contributions are expected to be negligible. This allows for the extraction of the non-resonant background which can then be used to make prediction for photon energies below 3 GeV. The deviation between the data and the prediction can then be interpreted as possible signatures for excited baryon resonances, particularly in the case of polarization observables and differential cross-section in the case of $\pi^-$ photoproduction from the neutron.

The observed enhancement might be associated with the strangeness production threshold [27,28]. They could also be related to the $\phi$-N bound state which has been predicted recently [29, 30]. The sudden drop in the scaled differential cross-section may shed light on the transition between the aforementioned physical pictures. To test the onset of the scaling behavior in charged photopion production process, and to understand the enhancement and the dramatic drop aforementioned, it is important to investigate the

detailed scaling behavior in a center-of-mass energy of 1.8 GeV to 2.5 GeV in very fine photon energy bins. Recently, we have carried out a detailed study of the differential cross-section of the $\gamma n \to \pi^- p$ process from a high statistics data sample obtained by the Jefferson Lab CLAS detector.

# 3 CLAS g10 analysis of the $\gamma n \to \pi^- p$ process

The experiment was carried out at the Thomas Jefferson National Accelerator Facility (Jefferson Lab) in Hall B with the CEBAF Large Acceptance Spectrometer (CLAS) [31]. The CLAS detector was designed to provide near $4\pi$ coverage of charged particles. Details about the CLAS can be found in Ref. [31]. For the CLAS g10 experiment [32], a 24 cm long liquid deuterium target was employed with the target cell positioned 25 cm upstream from the CLAS nominal center. A tagged photon beam was used which was generated by an electron beam with an incident beam energy of 3.8 GeV, corresponding to a maximum $\sqrt{s}$ of 2.8 GeV for the process of interest. The event trigger required at least two charged particles in different sectors. Two magnetic field settings were used during the experiment corresponding to a low-field setting (with torus current I=2250 A) and a high field setting (I=3375 A) which provided different angular coverage and momentum resolution. About 10 billion triggers were collected during the g10 running period of two months. The results from high field settings are consistent with those from the low field setting within systematic uncertainties.

The raw data collected from the experiment were first processed to calibrate and convert the information from the detector subsystem to physical variables such as energy, momentum, position and timing. This process generated about 40 Tera-bytes data. For the process of interest, the $\gamma n \to \pi^- p$ quasifree process from the deuteron, only events with one proton and one $\pi^-$ were selected. The vertex times of both proton and $\pi^-$ were required to be within 1 ns of the photon vertex time. For this quasifree process detected, only the neutron inside the deuteron was coupled to the photon, and the spectator proton was left intact. The spectator proton is usually moving with a momentum below 200 MeV/c, and is usually not detected by the CLAS. To select this channel from other background channels, the 4-momentum of the spectator proton is reconstructed by energy-momentum conservation. Only events with missing mass around the proton mass were selected to make sure the missing particle was the spectator proton. Further, a missing momentum cut of below 200 MeV/c was used in the analysis to select the quasifree events of $\gamma n \to \pi^- p$ from the deuterium target.

Monte Carlo simulations have been carried out to determine the accep-

tance and efficiency of the CLAS detector. Many practical factors, such as the geometry and inefficiencies of the detectors, result in loss of events during the experiment. This has to be recovered by simulations in order to extract cross sections. A virtual CLAS detector (GSIM) was built based on GEANT, which simulates an ideal CLAS detector with all the subsystem working perfectly. Millions of events were generated and passed through the GSIM and then the simulated data were processed to incorporate the subsystem efficiencies and resolutions extracted from the experiment. All the simulated data were then processed by the same softwares used in the real data processing and analysis. The ratio between the events passed the simulation and the generated events is the product of the acceptance and the efficiency of the detector. Since deuteron is used as an effective neutron target in this experiment, the final state interaction (FSI) effects must be taken into account before one extracts cross sections. The FSI correction is estimated according to the Glauber formulation [33] which relates the nuclear transparency to the total cross section of final state particle with nucleons inside the nucleus.

Preliminary CLAS g10 results suggest the approach of the scaling region in the more backward angle kinematics: 70° to 110°. They also confirm the existence of a broad resonance structure around a center-of-mass energy of 2.2 GeV at a pion center-of-mass angle of 90°. The preliminary results also confirm the drastic drop in differential cross-section by a factor of 15 in an energy window of about 300 MeV from 2.2 GeV to 2.5 GeV at 90°. Further, preliminary g10 results show a very interesting angular dependent resonance structure, i.e. the center-of-mass energy location of this resonance structure depends on the pion center-of-mass angle. Detailed analysis of the angular distribution of the data as a function of the center-of-mass energy will be carried out in the near future to better understand the nature of the observed resonance structure.

# Acknowledgments

I thank Bill Briscoe, Wei Chen, Dipangkar Dutta, Patrizia Rossi, A. Sibirtsev, Igor Strakovsky, Stepan Stepanyan, and Lingyan Zhu for helpful conversations. This work is supported in part by the U.S. Department of Energy under contract number DE-FG02-03ER41231.

# References

[1] S.J. Brodsky and G.R. Farrar, Phys. Rev. Lett.**31**, 1153 (1973); Phys. Rev. D **11**, 1309 (1975); V. Matveev *et al.*, Nuovo Cimento Lett. **7**, 719 (1973);

[2] R. L. Anderson *et al.*, Phys. Rev. D **14**, 679 (1976); C. White *et al.*, Phys. Rev. D **49**, 58 (1994).

[3] J. Napolitano *et al.*, Phys. Rev. Lett. **61**, 2530 (1988); S.J. Freedman *et al.*, Phys. Rev. C **48**, 1864 (1993); J.E. Belz *et al.*, Phys. Rev. Lett. **74**, 646 (1995).

[4] C. Bochna *et al.*, Phys. Rev. Lett. **81**, 4576 (1998).

[5] E.C. Schulte, *et al.*, Phys. Rev. Lett. **87**, 102302 (2001);

[6] P. Rossi *et al.*, Phys. Rev. Letts. **94**, 012301 (2005); M. Mirazita *et al.*, Phys. Rev. C **70**, 014005 (2004).

[7] K. Wijesooriya, *et al.*, Phys. Rev. Lett.86, 2975 (2001).

[8] H. Genzel, P. Joos, and W. Pfeil, Photoproduction of Elementary Particles (Springer-Verlag, Berlin, 1973), Group I Volume 8 of Numerical Data and Functional Relationships in Science and Technology, edited by K.-H. Hellwege.

[9] Q. Zhao and F. E. Close, Phys. Rev. Lett. **91**, 022004 (2003).

[10] X. Ji, J.-P. Ma and F. Yuan, Phys. Rev. Lett. **90**, 241601 (2003).

[11] J. Polchinski and M.J. Strassler, Phys. Rev. Lett. **88**, 031601 (2002); R.C. Brower and C.I. Tan, Nucl. Phys. B **662**, 393 (2003); O. Andreev, Phys. Rev. D **67**, 046001 (2003).

[12] S. J. Brodsky and G. F. de Teramond, Phys. Lett. **B582**, 211 (2004); S. J. Brodsky,J. R. Hiller, D. S. Hwang and V. A. Karmanov, Phys. Rev. D **69**, 076001 (2004).

[13] D. Dutta and H. Gao, Phys. Rev. C **71**, 032201(R) (2005).

[14] J. P. Ralston and B. Pire, Phys Rev. Lett. **49**, 1605 (1982); B. Pire and J. P. Ralston, Phys. Lett. B **117**, 233 (1982).

[15] G.R. Court *et al.*, Phys. Rev. Lett. **57**, 507 (1986);T.S. Bhatia *et al.*, Phys. Rev. Lett. **49**, 1135 (1982); E.A. Crosbie *et al.*, Phys. Rev. D **23**, 600 (1981).

[16] L. Y. Zhu *et al.*, Phys. Rev. Lett. **91**, 022003 (2003); L. Y. Zhu *et al.* Phys Rev. C, **71**, 044603 ( 2005).

[17] J. Alcorn *et al.*, Nucl. Instrum. Methods A522, 294 (2004).

[18] P. Ulmer *et al.*, http://www.physics.odu.edu/∼ulmer/mceep/mceep.html.

[19] L.Y. Zhu, Ph.D. thesis, February, 2004, Massachusetts Institute of Technology (unpublished).

[20] M. Dugger *et al.*, Phys. Rev. C **76**, 025211 (2007).

[21] http://pdg.lbl.gov/2007/hadronic-xsections/hadronicrpp_page13.pdf.

[22] The GWU CNS Database, http://gwdac.phys.gwu.edu/analysis/pr_analysis.html

[23] S. Capstick, Phys. Rev. D **46**, 2864 (1992); S. Capstick and W. Roberts, Phys. Rev. D **49**, 4570 (1994).

[24] O. Bartholomy *et al.*, Phys. Rev. Lett **94**, 012003 (2005).

[25] V. Crede *et al.*, Phys. Rev. Lett **94**, 012004 (2005).

[26] A. Sibirtsev, J. Haidenbauer, S. Krewald, T.-S.H. Lee, U.-G. Meissner, and A.G. Thomas, Nucl-th/07060183.

[27] S. J. Brodsky, and G. F. de Teramond, Phys. Rev. Lett. **60**, 1924 (1988).

[28] S.J. Brodsky, I.A. Schmidt, G.F. de Teramond, Phys. Rev. Lett. **64**, 1011 (1990).

[29] H. Gao, T.S.-H. Lee, and V. Marinov, Phys. Rev. C **63**, 022201(R) (2001).

[30] F. Huang, Z.Y. Zhang, and Y.W. Yu, Phys. Rev. C **73**, 025207 (2006).

[31] B. Mecking and the CLAS Collaboration, The Cebaf Large Acceptance Spectrometer, *Nucl. Instr. & Meth.* **503/3** 513 (2003)

[32] B. McKinnon, K. Hicks *et al.*, Phys. Rev. Lett. **96**, 212001 (2006); S. Niccolai, M. Mirazita, P. Rossi *et al.*, Phys. Rev. Lett. **97**, 032001 (2006).

[33] H. Gao, R.J. Holt, and V.R. Pandharipande, Phys. Rev. C **54**,2779 (1996).